Tetrahedron 67 (2011) 48–57

Contents lists available at ScienceDirect

Tetrahedron

journal homepage: www.elsevier.com/locate/tet

Hydrogen bonded arylamide-linked cholesteryl dimesogenic liquid crystals: a study of the length and side chain effects

Gui-Tao Wang, Xin Zhao, Zhan-Ting Li *

State Key Laboratory of Bioorganic and Natural Products Chemistry, Shanghai Institute of Organic Chemistry, Chinese Academy of Sciences, 345 Lingling Lu, Shanghai 200032, China

ARTICLE INFO

Article history:
Received 18 September 2010
Received in revised form 4 November 2010
Accepted 9 November 2010
Available online 13 November 2010

Keywords:
Hydrogen bond
Foldamer
Cholesterol
Aromatic amide
Liquid crystal

ABSTRACT

Dimesogenic compounds **1a**–**c**, **2a**–**i**, and **3**, that are composed of a hydrogen bonding-induced straight arylamide spacer and two appended cholesterol groups, have been designed and synthesized. The backbones of the rigid spacers of **1a**–**c**, **2a**–**i**, and **3** contain one, three, and five benzene units, which bear two, six, and ten alkoxyl (methoxyl, *n*-octoxyl, or *n*-dodecoxyl) groups, respectively. The thermal and optical properties of the compounds are investigated by using the differential scanning calorimetry (DSC), polarizing optical microscopy (POM), and powder X-ray diffraction (PXRD) analysis. It is revealed that **1a**–**c** exhibit one or two liquid crystalline (LC) phases, **2a**–**i** exhibit no, one or two LC phases, while **3** exhibits one LC phase in a wide temperature range. Generally, the more and longer alkoxyl chains facilitate the formation of the LC phases at low temperature. Notably, compound **2g**, which bears two methoxyl and four dodecoxyl groups, displays a blue-red color change during both the heating and cooling cycle. The result illustrates that dimesogens with large rigid spacers can exhibit different LC phases when long aliphatic chains are appended to balance the strong stacking of the rigid backbones.

1. Introduction

Liquid crystals (LCs) are compounds, which exhibit both the properties of a well arranged crystal and highly disordered liquid state.[1–16] In recent years, dimesogenic LCs that consist of two mesogenic units and a linking spacer have attracted considerable attention because they not only show new unique optical property, but also serve as useful models for semi-rigid main-chain LC polymers.[2] One major family of dimesogens is those containing two peripheral cholesteryl groups, which have been extensively investigated for the structure–property relationships.[12–16] In most cases, the cholesteryl groups are linked by a flexible spacer, normally an aliphatic chain. Small rigid units, such as diyne,[17,18] benzene[19] or biphenyl,[20] have also been incorporated into the flexible spacers, which showed that the rigidity of the spacer and its intermolecular interactions dramatically affect the thermal and optical properties of cholesterol-based dimesogens. However, investigations on the effect of larger rigid, conjugated spacers on the LC property of cholesterol-derived dimesogens have not been available probably because of the fact that large side chain-free conjugated systems usually stack strongly, which may unfavor the liquid feature required for the formation of an LC phase.

Hydrogen bonded arylamide foldamers have well-defined conformations due to the strength and directionality of their intramolecular hydrogen bonding and the intrinsic rigidity and planarity of the benzamide unit.[21–24] Thus, our group has had a longstanding interest in developing functional materials from this family of preorganized backbones.[25,26] For example, porphyrin-appended folded arylamide backbones can entrap fullerenes or their derivatives to generate new supramolecular LCs.[27,28] Herein, we report the LC properties of a new class of dimesogens that are composed of a large hydrogen bonded preorganized oligomeric arylamide spacer and two appended cholesteryl groups, especially from the viewpoint of the length and side chain effect of the rigid spacer on the thermal and optical behaviors of the dimesogenic compounds.

2. Results and discussion

Compounds **1a**–**c**, **2a**–**i**, and **3** were designed and prepared. The intramolecular five- and six-membered hydrogen bonds shown in the structures have been well-established.[21–24] The aromatic backbones of trimers **2a**–**i** and pentamer **3** possess straight conformations due to the formation of the intramolecular hydrogen bonding.[29,30] The two cholesterol groups were introduced to the two ends of these rigid spacers to test the effect of large conjugated segments on the LC property of the resulting dimesogens. Aliphatic chains, including methyl, *n*-octyl, and dodecyl, were appended to the backbones from the two sides of the spacers. These chains were designed not only to tune the solubility of the new dimesogens, but also, more importantly, for a systematical investigation of their influence on the LC property. For comparison, compound **4** was also prepared.

The synthetic routes for the new dimesogens are provided in Scheme 1. Compounds **5a**–**c** were first mononitrated to give **6a**–**c**

* Corresponding author. Tel.: +86 21 54925122; fax: +86 21 64166128; e-mail address: ztli@mail.sioc.ac.cn (Z.-T. Li).

0040-4020/$ – see front matter © 2010 Elsevier Ltd. All rights reserved.
doi:10.1016/j.tet.2010.11.046

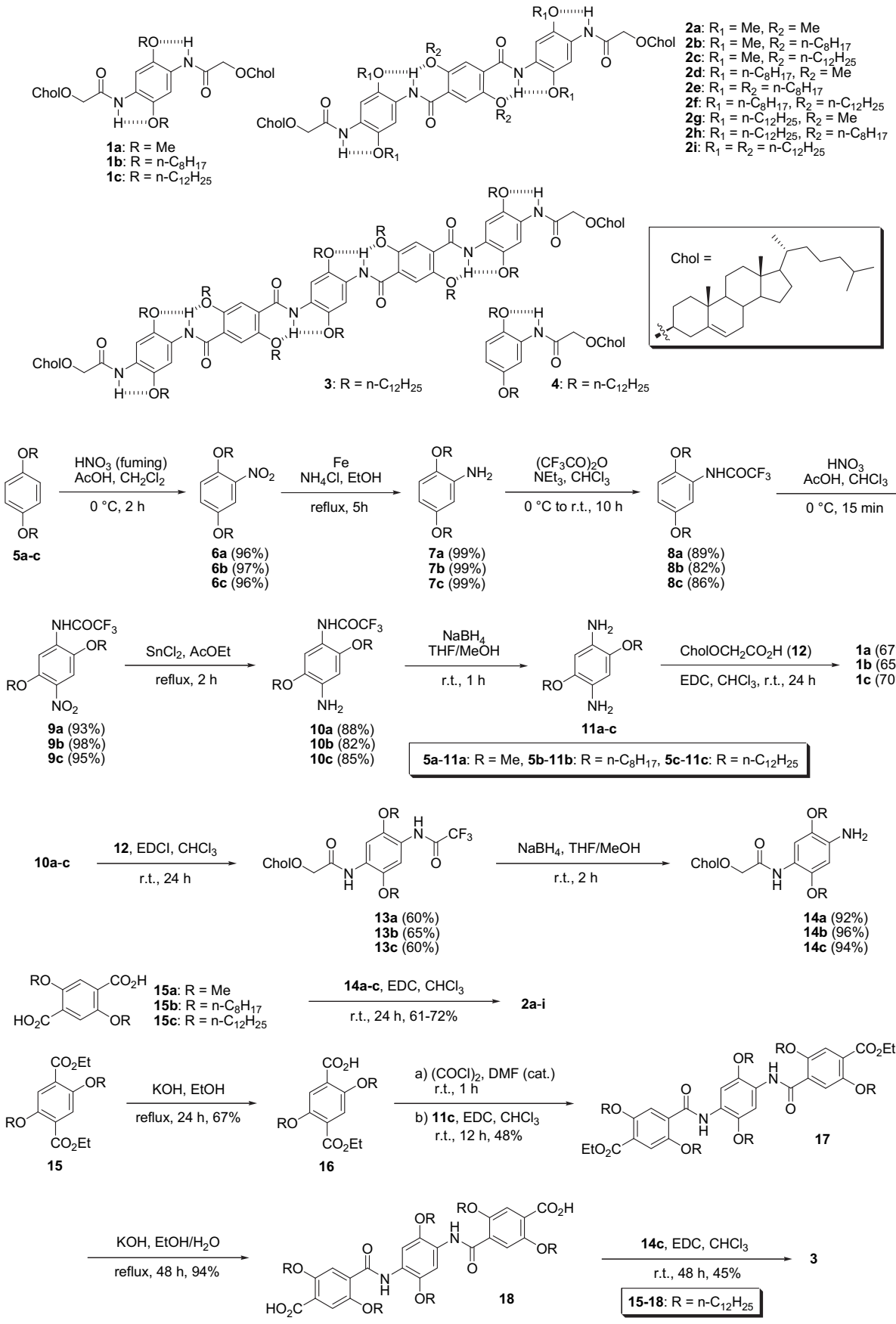

Scheme 1. Synthesis of compounds **1a**–**c**, **2a**–**i**, and **3**.

in 96–97% yields. Dinitration of **5a**–**c** with nitric acid always produced a mixture of 2,3- and 2,5-dinitro isomers.[31] The mononitrates were reduced with iron powder and ammonium chloride to **7a**–**c** quantitatively. Treatment of the anilines with trifluoroacetic anhydride to afford **8a**–**c** in 82–88% yields. The amides were then further nitrated in acetic acid to give **9a**–**c** in 93–98% yields. These nitrates were then treated with stannous chloride to give **10a**–**c** in 82–88% yields. Treatment of compounds **10a**–**c** with sodium borohydride afforded diamines **11a**–**c**, which were further coupled with acid **12**[32] to produced **1a**–**c** in 65–70% yields. For the synthesis of **2a**–**i**, **10a**–**c** were first coupled with **12** to produce **13a**–**c** in 60–65% yields. These diamides were then treated with sodium borohydride to afford **14a**–**c** in 92–96% yields. These anilines were further coupled with diacids **15a**–**c** to give **2a**–**i** in 61–72% yields. For the preparation of pentamer **3**, compound **15** was first hydrolyzed with potassium hydroxide to give **16** in 67% yield. The acid was then coupled with **11c** to afford **17** in 48% yield. The diester was further treated with potassium hydroxide to afford **18** in 94% yield. Finally, the diacid was coupled with **14c** to produce **3** in 45% yield. Compound **4** was prepared in 56% yield from the reaction of **7c** and **12**. All the compounds are soluble in chloroform and their ^{1}H NMR spectra in chloroform-*d* were of good resolution. The signals of their amide protons all appeared in the downfield field (≥9.10 ppm), supporting that these protons were involved in the intramolecular hydrogen bonding.

The mesomorphic properties of the above compounds were investigated using polarized optical microscopy (POM). The phase transition temperatures were estimated by differential scanning calorimetry (DSC). Table 1 summarizes their thermal behavior and enthalpy changes that were collected from the DSC thermograms.

Table 1
Phase transition temperatures and enthalpies of compounds **1a**–**c**, **2a**–**i**, and **3**

	Phase transition temperatures/°C (ΔH/kJ mol^{-1})[a]	
	Heating	Cooling
1a	Cr 206 (42.7) N* 300 dec	
1b	Cr 72 (10.5) ordSm 230 (39.4) I	I 218 (−4.4) N* 199 (−35.5) ordSm 60 (−6.8) Cr
1c	Cr 193 (33.5) ordSm 205 (52.7) I	I 205 (−5.0) N* 193 (−41.4) ordSm 174 (−34.0) Cr
2a	Cr >300[b]	
2b	Cr 270 (98.7) I	I 252 (−70.0) Cr
2c	Cr 243 (89.2) I	I 229 (−76.0) Cr
2d	Cr 233 (49.3) I	I 221 (−47.1) Cr
2e	Cr 175 (52.6) I	I 164 (−52.2) Cr
2f	Cr 160 (52.6) I	I 153 (−25.1) Sm 112 (−20.7) Cr
2g	Cr 89 (7.4) Cr′ 106 (3.2) ordSm 205 (46.5) I	I 195 (−46.5) ordSm 89 (−2.2) Cr′ 72 (−8.2) Cr
2h	Cr 123 (3.5) ordSm 142 (10.5) N* 155 (17.6) I	I 151 (23.7) N* 119 (8.8) ordSm 86 (5.7) Cr
2i	Cr 103 (52.8) ordSm 156 (49.5) I	I 152.2 N* 150 ordSm 80 (−60.6) Cr
3	Cr 104 (55.4) Cr′ 191 (83.7) I	I 183 (−83.3) Sm 80 (−102.0) Cr
4	Cr 121 (1.26) I	I 120 (−1.23) Cr

[a] dec: decomposed; Cr, Cr′: crystalline; N*: chiral nematic; Sm: fluid smectic; ordSm: ordered smectic; I: isotropic liquid.
[b] Mp >300 °C.

DSC indicated that, upon heating or cooling, compound **4** exhibited a phase transition between the crystalline state and the isotropic liquid state. POM also showed that it melted directly into an isotropic liquid.

Compound **1a** melted at 206 °C to exhibit an oil streak texture, indicating the presence of a chiral nematic (N*) phase (Fig. 1a).[33] Further heating to 300 °C did not lead to a clear point. Thermogravimetric analysis (TGA) indicated that the sample began to decompose at this temperature (see Supplementary data, Fig. S1a). Thus, an investigation of its phase transition at cooling was not performed.

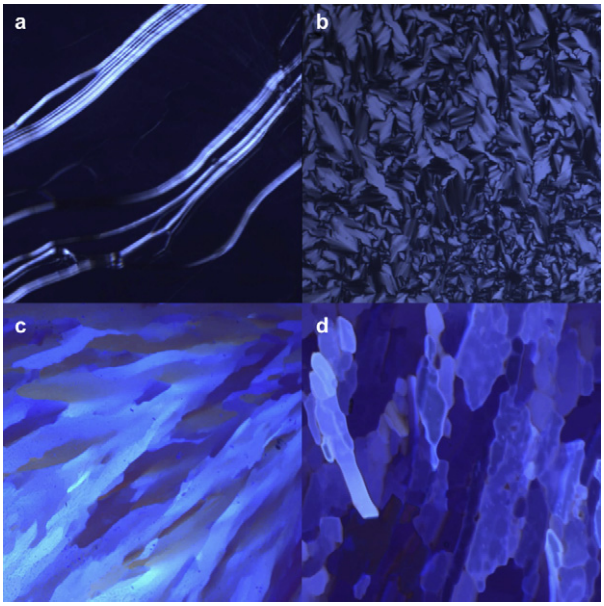

Fig. 1. (a) The POM texture (oil steak) of **1a** at 250 °C on heating, the POM textures of **1c** (b–d) fan-like: 205 °C on cooling; mosaic: 190 °C on cooling; mosaic: 195 °C on heating.

Compound **1c**, which bears two *n*-dodecyloxyl groups at the centrally positioned benzene ring, melted into an isotropic liquid at 205 °C. This temperature is considerably lower than that of **1a**, which is consistent with the fact that flexible aliphatic chains weaken the stacking of the rigid cholesterol and aromatic moieties. The DSC thermograms of **1c** registered upon cooling showed three sharp exothermic peaks. Its POM showed that the first peak was related to the transition of the liquid state to an LC state that had a fan-like texture (Fig. 1b). The PXRD profile of the LC state was very similar to that obtained in the liquid state, with no diffraction peaks observed in the small-angle area of the PXRD profile (Fig. 2a), suggesting the formation of a chiral nematic phase.[30,31] The second peak was related to the formation of another LC phase with a mosaic texture (Fig. 1c). Its PXRD profile (190 °C) exhibited a sharp diffraction peak (2θ=3.52°, d=2.5 nm), which could be indexed as (001) of the lamellar structure (Fig. 2b).[34] Molecular modeling revealed that, when adopting an extended conformation, the backbone of **1c** had a length of ca. 4.2 nm. Thus, the above layer

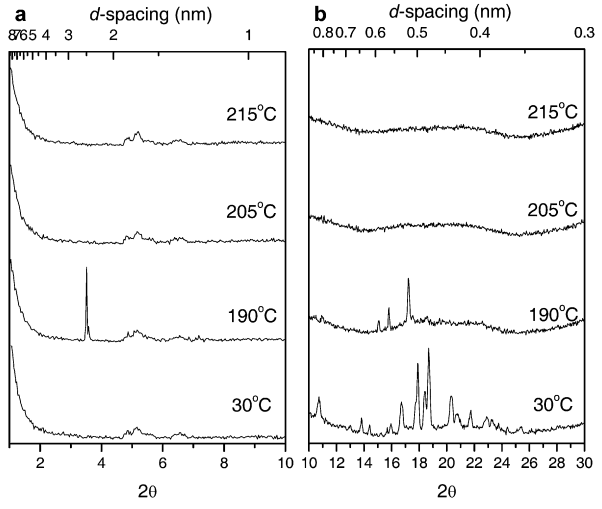

Fig. 2. The PXRD pattern of compound **1c** at various temperatures on cooling, 2θ in range of (a) 1°–10° and (b) 10°–30°.

spacing supported that this compound adopted an interlayered stacking pattern, as shown in Fig. 3a, and the cholesterol moiety had only a small inclination. The interlayer space between the separated aromatic rings should be filled by the aliphatic chains. Upon cooling to 174 °C, **1c** turned into the crystalline state. For the heating cycle, the chiral nematic phase was not exhibited. Instead, the ordered smectic phase was directly changed to the liquid phase at 205 °C. The phase transition behavior of compound **1b** (see Supplementary data, Fig. S2) was very similar to that of **1c**. The PXRD profile of the ordered smectic phase of **1b** also displayed a sharp diffraction peak, albeit corresponding to a smaller layer spacing (2.1 nm) (see Supplementary data, Fig. S3), which might be attributed to that the shorter *n*-octyl chains allowed for a closer intermolecular stacking of the large cholesterol segments.

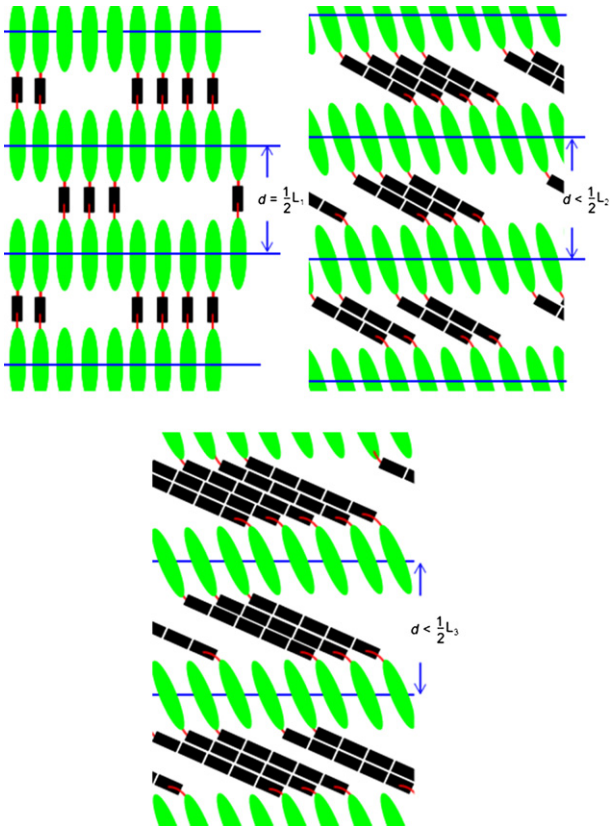

Fig. 3. Proposed stacking patterns in the ordered smectic phase of **1** (upper, left), **2** (upper, right), and **3** (down). The cholesterol group, arylamide spacer, and linker were represented by green ellipse, black rectangles, and red lines, respectively. The side chains, which should fill the space between the separated aromatic segments, were omitted for clarity.

Compounds **2a**–**i** possessed the identical large aromatic amide spacer of three benzene rings. The aromatic spacers were expected to stack strongly. The modulation of the six alkoxyl groups on the thermal and optical properties of this series of compounds was then investigated. Compound **2a**, which, like **1a**, bears two methoxyl groups, did not melt, but decomposed at 300 °C (see Supplementary data, Fig. S1b), reflecting an increased crystallization as a result of the enlarged aromatic segment. The DSC experiments showed that compounds **2b**–**e** exhibited only one endothermic peak, from the heating cycle, and one exothermic peak, from the cooling cycle, suggesting no formation of the LC phase. Clearly the longer aromatic linkers enhanced intermolecular ordered stacking and thus reduced their capacity of forming LC phase. For both the heating and cooling cycles, the melting temperature of compound **2e**, which bears 6 *n*-octoxyl groups of totally 48 carbons, was considerably lower than that of **2b**–**d**, bearing alkoxyl groups of from 20 to 36 carbons. This observation indicated that the introduction of more and longer side chains also more strongly weakened the stacking of the aromatic spacer. POM experiment also revealed that, when the liquid state was cooled at a very low rate (1 °C/min), **2e** exhibited a chiral nematic LC phase at a very narrow temperature (<0.5 °C) before the formation of the crystalline phase (see Supplementary data, Fig. S4a). Although no PXRD analysis was available due to the very narrow temperature range, this result appeared to indicate that more and longer chains would help to induce the formation of a more stable liquid crystal phase for this series of molecules with large rigid aromatic linkers.

Compared with that of **2e**, the melting temperature of compound **2f** was further decreased due to the presence of the two longer *n*-dodecyl chains. Although no LC phase was observed from the heating cycle, upon cooling **2f** exhibited an LC phase within the temperature range of 153–112 °C (see Supplementary data, Fig. S4b). The fan-like texture related to a chiral smectic phase and equidistant line pattern could be observed from the texture. The PXRD profile of **2f** displayed a sharp diffraction peak at 2θ=3.91° (see Supplementary data, Fig. S5a,b), which corresponded to a layer spacing of 2.3 nm and also suggested the existence of the smectic LC phase. Because molecular modeling showed that the backbone of **2f** had a length of ca. 5.7 nm in its extended state, this distance suggested that the molecule should be arranged in a slipped-stacking order with the cholesterol groups also aggregating alternatively, as shown in Fig. 3b.

Compound **2g** exhibited LC states from both the heating and cooling cycles. For the cooling cycle, the transition from the liquid phase to the LC phase occurred at 206 °C as determined by DSC. In particular, the color of the LC texture changed gradually from red to purple, and then to blue at the very beginning of the transition to the LC phase. Upon further cooling, the wavelength of the color started to increase and went back to light red (Fig. 4a–e, also see Supplementary data, Fig. S6). The texture further changed its color to dark green at even lower temperature close to the melting point (Fig. 4f). This result reflected that the compound appeared to form

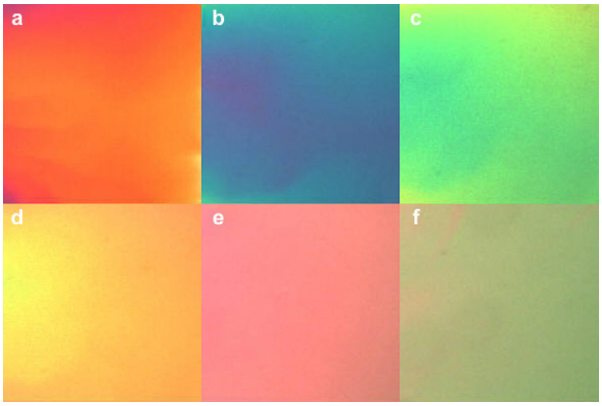

Fig. 4. The POM textures of **2g**, on cooling, at (a) 209.2 °C, (b) 208.6 °C, (c) 207.5 °C, (d) 206.4 °C, (e) 189.6 °C, and (f) 103.1 °C, revealing temperature-dependent color change.

a helical super-structure.[16] The pitch length of the cholesterol groups in the helix was increased with temperature, and thus induced the shifting of the color with temperature. A reverse color change was also observed from the heating cycle, and the process could be repeated. Upon cooling to below 180 °C, the PXRD profile of **2g** exhibited a sharp peak in the small-angle area (2θ=2.76°, d=3.2 nm) (Fig. 5), indicating the existence of a lamellar structure. This layer spacing was also considerably smaller than the length of its extended backbone. Thus, **2g** might also adopt a stacking pattern similar to that of **2f** but with a reduced dislocation (Fig. 3b). Several

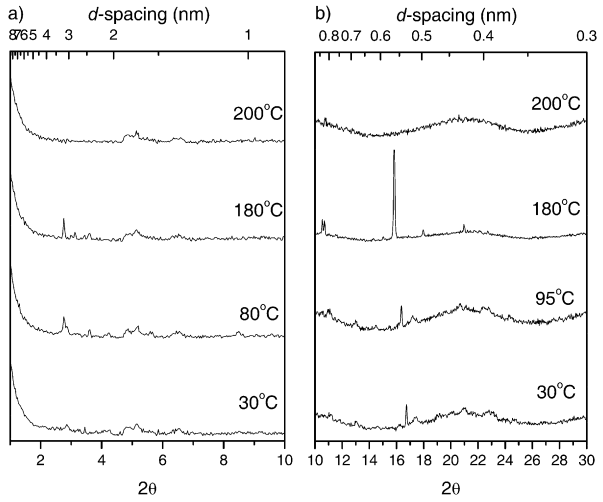

Fig. 5. The PXRD pattern of compound **2g** at various temperatures on cooling, 2θ in range of (a) 1°–10° and (b) 10°–30°.

peaks in the wide-angle area were also observed for **2g**, which implied that there might also exist ordered arrangements for the cholesterol moieties within the layer.

Upon cooling to 151 °C, compound **2h**, which bears four *n*-octoxyl and two *n*-dodecyloxyl chains, underwent a transition from the liquid phase to the LC phase of a fan-like texture (see Supplementary data, Fig. S4c). The PXRD did not exhibit any peaks in the small-angle area that corresponded to the spacing of layers (see Supplementary data, Fig. S5c,d). Thus, this texture should also be a chiral nematic phase. Below 119 °C, it changed to a smectic LC phase that had a mosaic texture (see Supplementary data, Fig. S4d). For the cooling cycle, **2i**, bearing six *n*-dodecyloxyl chains, underwent a transition from the liquid phase to the LC phase at 152 °C. The texture of this LC phase also exhibited the equidistant line pattern (see Supplementary data, Fig. S4f). This LC phase had a narrow temperature area of only 2 °C and probably was also a chiral nematic phase. Upon cooling to 150 °C, it changed to an ordered smectic LC phase with a mosaic texture (see Supplementary data, Fig. S4g). The PXRD profiles at 100 °C revealed a layer spacing of 2.4 nm (2θ=3.69°) for both **2h** and **2i** (see Supplementary data, Fig. S5c–f), suggesting that they had the identical dislocated stacking pattern (Fig. 3b). We may propose that the difference of the size of the two centrally appended aliphatic chains was not great enough to affect the stacking pattern of the whole skeleton of the two molecules. For the heating cycle, the phase transition behavior of **2h** was inverse to that of the cooling cycle, although a hysteresis was always observed for the transition. In contrast, the heating cycle of **2i** exhibited only one ordered smectic LC phase, which directly melted into the liquid phase upon further heating.

The above results of **2a**–**i** indicated that, for the dimesogens with a large rigid aromatic spacer, introduction of more and longer side chains to the centrally positioned aromatic segments may balance the strong stacking interaction of the spacers and lead to the formation of the LC phase. However, no simple linear relationship was observed because the effect of the appended chains was affected by many factors such as their length, position, and the stacking of both the spacer and the cholesterol groups. Compared to **1a**–**c**, **2a**–**i** have more side chains with different arrangements, which enabled the creation of discrete kinds of LC properties. It was also noted that, although **2e** and **2f** are different only for the two centrally appended chains, they exhibited very different LC properties. In contrast, the similar difference between **1b** and **1c** and **2h** and **2i** resulted in only a slight change of the LC properties, reflecting the complexity for the effect of the appended chains on the stacking and LC properties of the dimesogens.

Compound **3** has the longest spacer of 5 aromatic units, which are attached with 10 *n*-dodecyloxyl chains. For the heating cycle, no LC phase was exhibited, although it exhibited two crystalline phases. The compound melted into an isotropic liquid at 191 °C. Upon cooling to 183 °C, **3** changed from the liquid phase to a smectic LC phase that had a fan-like texture (Fig. 6). The LC phase lasted until the temperature was decreased to 80 °C. The PXRD profile at 180 °C exhibited a sharp diffraction peak in the small-angle area (2θ=3.19°, d=2.8 nm) (Fig. 7). This spacing of layers was remarkably smaller than the length of its backbone, indicating that it might adopt a stacking pattern similar to the above trimer series, but with a larger dislocation for both the cholesterol and aromatic spacer (Fig. 3c). The melting point of **3** was higher than that of **2i**, but lower than that of **1c**. All the three molecules bear the longest *n*-dodecyloxyl chains, but have spacers of varying length. The result appeared to indicate that the stacking interaction of the rigid backbone and the thermal motion of the chains of **2i** reached the 'best' balance for the lowest transition temperature. Notably, compound **3** displayed the widest temperature range of larger than 100 °C for the LC phase, which should be attributed to the longest

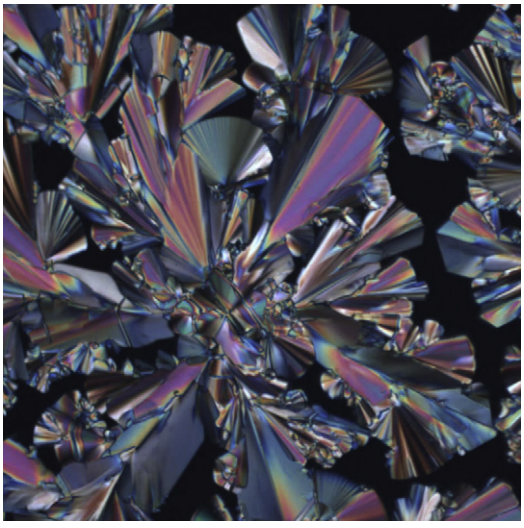

Fig. 6. The POM texture (fan-like) of compound **3** at 187 °C on cooling.

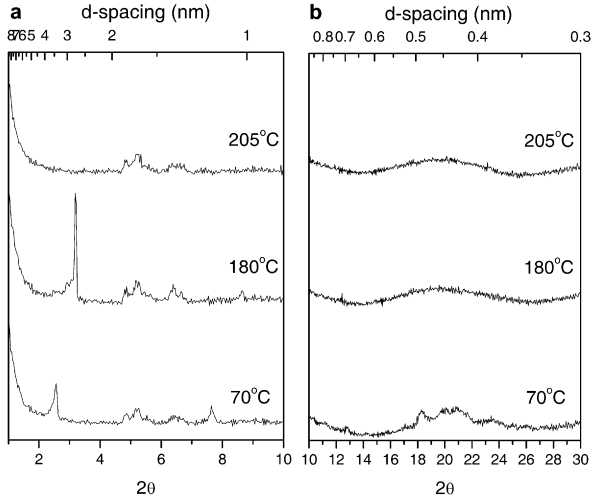

Fig. 7. The PXRD pattern of compound **3** at various temperatures on cooling, 2θ in range of (a) 1°–10° and (b) 10°–30°.

aromatic spacer. Its large dimension and the ten appended *n*-dodecyloxyl chains enabled the whole molecule to maintain the identical stacking pattern within a wide range of temperature. Compound **1b** kept the LC phases within a slightly wider temperature range. However, **1b** had a transition between two LC phases and displayed more crystal-like ordered smectic phase, while **3** exhibited only a single fluid smectic phase.

3. Conclusion

A new family of dimesogens that consist of a rigid arylamide spacer and two peripheral cholesterol groups has been designed and synthesized. Their thermal and optical properties are systematically investigated. The result illustrates that dimesogens with large rigid spacers can exhibit different LC phases if long aliphatic chains are appended to balance the strong stacking of the rigid backbones.

Because the conformations of the rigid aromatic backbones can be readily modulated by changing the position of the substituents, the shape effect of the spacer may also be investigated. The cholesterol or other mesogenic groups may be introduced to the hydrogen bonded spacers from the two sides. In this way, new liquid crystals that are structurally similar to the side chain polymer liquid crystals may be developed.

4. Experimental section

4.1. General methods

All reagents were obtained from commercial sources and used without further purification. The solvents have been purified by using standard procedures before use. Silica gel (10–40 μ) was used for all column chromatography. Analytical thin-layer chromatography (TLC) was performed on 0.2 mm silica 60 coated on glass plates with F_{254} indicator. The NMR spectra were recorded on a 300 or 400 MHz spectrometer in the indicated solvent. Chemical shifts are expressed in parts per million (δ) using residual proton resonances of the deuterated solvents as the internal standards. The mass spectra were gathered on an HP 5989A or a Bruker Daltonics FTMS-7 instrument. Differential scanning calorimetry (DSC) was recorded on Pyris-1 (Perkin Elmer Co) instrument, which was calibrated with indium; the scanning rate was 10 °C/min and the samples were sealed in aluminum capsules in the air. For thermogravimetric analysis (TGA), a Q500 instrument (TA Co) was used. Microscopic studies were carried out using an Olympus BX51 polarized optical microscope equipped with Linkam LTS350 thermal stage. The XRD patterns were obtained on X′Pert Pro MPD (Panalytical Co), and the sample was filled in Lindemann capillaries of ca. 1 mm diameter. The energy minimized conformation was obtained by molecular dynamic simulation using MMFF force field.

4.2. Compounds 8a–c

To a stirred solution of compound **7b** (17.9 g, 51.0 mmol) in chloroform (100 mL) and triethylamine (6.20 g, 61.0 mmol), cooled in an ice-bath, was slowly added a solution of trifluoroacetic anhydride (11.7 g, 56.0 mmol) in chloroform (200 mL). The mixture was stirred at room temperature for 10 h and then washed with diluted hydrochloric acid (0.5 N, 100 mL), water (2×100 mL), and brine (100 mL), and dried over sodium sulfate. Upon removal of the solvent with a rotavapor, the crude product was recrystallized from petroleum ether (60–90 °C) to give compound **8b** as a white solid (18.6 g, 82%). ^{1}H NMR (300 MHz, $CDCl_3$): δ 8.65 (s, 1H), 7.98 (d, J=3.0 Hz, 1H), 6.83 (d, J=9.0 Hz, 1H), 6.67 (dd, J_1=9.0 Hz, J_2=3.0 Hz, 1H), 4.01 (t, J=7.5 Hz, 2H), 3.93 (t, J=7.5 Hz, 2H), 1.83–1.73 (m, 4H), 1.45–1.29 (m, 20H), 0.91–0.87 (m, 6H). ^{13}C NMR (100 MHz, $CDCl_3$): δ 154.0 (q, J=38 Hz), 153.3, 141.7, 125.7, 115.6 (q, J=287 Hz), 112.2, 111.5, 106.8, 69.5, 68.7, 31.8, 31.7, 29.3 (d), 29.2 (d), 26.0 (d), 22.7, 22.6, 14.1, 14.0. ^{19}F NMR (282 MHz, $CDCl_3$): δ −76.4 (s). MS (ESI): m/z 446 $[M+H]^+$, 463 $[M+H_2O]^+$. Anal. Calcd for $C_{24}H_{38}F_3NO_3$: C, 64.70; H, 8.60; N, 3.14. Found: C, 64.81; H, 8.60; N, 3.29.

*4.2.1. Compound **8a**.* White solid. ^{1}H NMR (300 MHz, $CDCl_3$): δ 8.58 (s, 1H), 8.00 (d, J=3.0 Hz, 1H), 6.84 (d, J=9.0 Hz, 1H), 6.69 (dd, J_1=9.0 Hz, J_2=3.0 Hz, 1H), 3.88 (s, 3H), 3.78 (s, 3H). ^{19}F NMR (282 MHz, $CDCl_3$): δ −76.3 (s). MS (ESI): m/z 250 $[M+H]^+$, 267 $[M+H_2O]^+$.

*4.2.2. Compound **8c**.* ^{1}H NMR (300 MHz, $CDCl_3$): δ 8.66 (s, 1H), 7.98 (d, J=3.0 Hz, 1H), 6.83 (d, J=9.0 Hz, 1H), 6.67 (dd, J_1=9.0 Hz, J_2=3.0 Hz, 1H), 4.00 (t, J=7.5 Hz, 2H), 3.92 (t, J=7.5 Hz, 2H), 1.83–1.73 (m, 4H), 1.45–1.29 (m, 36H), 0.91–0.87 (m, 6H). ^{13}C NMR (100 MHz, $CDCl_3$): δ 154.2 (q, J=38 Hz), 153.3, 141.7, 125.7, 115.7 (q, J=287 Hz), 112.3, 111.5, 106.8, 69.5, 68.7, 31.9, 29.7, 29.6 (d), 29.5, 29.4, 29.3 (d), 29.2, 26.0, 22.7, 14.1. ^{19}F NMR (282 MHz, $CDCl_3$): δ −76.4 (s). MS (ESI): m/z 558 $[M+H]^+$, 575 $[M+H_2O]^+$. Anal. Calcd for $C_{32}H_{54}F_3NO_3$: C, 68.91; H, 9.76; N, 2.51. Found: C, 68.86; H, 9.97; N, 2.23.

4.3. Compounds 9a–c

To a stirred solution of compound **8b** (17.8 g, 40.0 mmol) in chloroform (100 mL) and acetic acid (50 mL), cooled in an ice-bath, was added fume nitric acid (98%, 25 mL) dropwise. The solution was stirred for 15 min and then poured to ice water (200 mL). The organic phase was separated and the aqueous phase extracted with chloroform (2×100 mL). The organic phases were combined and washed with aqueous sodium bicarbonate solution (0.5 N, 2×100 mL), water (2×100 mL), brine (100 mL), and dried over sodium sulfate. After the solvent was evaporated, the resulting residue was recrystallized from ethyl acetate to give compound **9b** as a yellow solid (19.2 g, 98%). ^{1}H NMR (300 MHz, $CDCl_3$): δ 8.75 (s, 1H), 8.25 (s, 1H), 7.53 (s, 1H), 4.13–4.07 (m, 4H), 1.88–1.81 (m, 4H), 1.49–1.29 (m, 20H), 0.91–0.86 (m, 6H). ^{13}C NMR (100 MHz, $CDCl_3$): δ 154.7 (q, J=38 Hz), 148.3, 140.3, 134.7, 130.5, 115.3 (q, J=287 Hz), 108.5, 106.3, 70.4, 70.0, 31.7, 31.6, 29.14, 29.10, 28.9, 28.8, 25.8, 25.7, 22.6, 22.5, 14.0, 13.9. ^{19}F NMR (282 MHz, $CDCl_3$): δ −76.4 (s). MS (ESI): m/z 491 $[M+H]^+$. Anal. Calcd for $C_{24}H_{37}F_3N_2O_5$: C, 58.76; H, 7.60; N, 5.71. Found: C, 58.75; H, 7.54; N, 5.58.

*4.3.1. Compound **9a**.* Yellow solid. ^{1}H NMR (300 MHz, $CDCl_3$): δ 8.71 (s, 1H), 8.30 (s, 1H), 7.57 (s, 1H), 3.97 (s, 6H). ^{13}C NMR (100 MHz, $CDCl_3$): δ 154.8 (q, J=38 Hz), 148.8, 141.0, 134.3, 130.5, 115.2 (q, J=286 Hz), 107.7, 105.4, 57.0, 56.6. ^{19}F NMR (282 MHz, CDCl3): δ −76.2 (s). MS (ESI): m/z 295 $[M+H]^+$. Anal. Calcd for $C_{10}H_9F_3N_2O_5$: C, 40.83; H, 3.08; N, 9.52. Found: C, 40.77; H, 3.13; N, 9.58.

*4.3.2. Compound **9c**.* Yellow solid. ^{1}H NMR (300 MHz, $CDCl_3$): δ 8.76 (s, 1H), 8.25 (s, 1H), 7.53 (s, 1H), 4.12–4.07 (m, 4H), 1.90–1.79 (m, 4H), 1.49–1.29 (m, 36H), 0.90–0.85 (m, 6H). ^{13}C NMR (100 MHz, $CDCl_3$): δ 154.8 (q, J=38 Hz), 148.4, 140.3, 134.8, 130.5, 115.3 (q, J=287 Hz), 108.6, 106.2, 70.4, 70.0, 31.9, 29.6 (d), 29.5, 29.3 (d), 29.2, 28.9, 28.8, 25.9, 25.8, 22.6, 14.0. ^{19}F NMR (282 MHz, $CDCl_3$): δ −76.4 (s). MS (ESI): m/z 603 $[M+H]^+$. Anal. Calcd for $C_{32}H_{53}F_3N_2O_5$: C, 63.76; H, 8.86; N, 4.65. Found: C, 63.29; H, 8.60; N, 4.54.

4.4. Compounds 10a–c

A suspension of compound **9b** (0.83 g, 1.70 mmol) and stannous chloride monohydrate (2.10 g, 10.0 mmol) in ethyl acetate (20 mL) was stirred under reflux for 2 h and then cooled to room temperature. Saturated aqueous sodium bicarbonate solution was added dropwise to pH=8. The formed solid was filtrated off with Celite.

The organic phase was separated and the aqueous phase extracted with ethyl acetate (20 mL). The organic phases were combined and washed with water (2×20 mL) and brine (20 mL) and dried over sodium sulfate. The solvent was then evaporated and the obtained slurry recrystallized from ethanol to give compound **10b** as a white solid (0.64 g, 82%). ^{1}H NMR (300 MHz, $CDCl_3$): δ 8.47 (s, 1H), 7.88 (s, 1H), 6.35 (s, 1H), 3.99–3.87 (m, 6H), 1.82–1.73 (m, 4H), 1.44–1.28 (m, 20H), 0.90–0.86 (m, 6H). ^{13}C NMR (100 MHz, $CDCl_3$): δ 153.4 (q, J=37 Hz), 142.5, 139.9, 134.3, 115.9 (q, J=286 Hz), 115.7, 105.3, 99.8, 69.4, 69.1, 31.7, 31.6, 29.3 (d), 29.2 (d), 29.1, 26.0 (d), 22.6 (d), 14.0 (d). ^{19}F NMR (282 MHz, $CDCl_3$): δ −76.3 (s). MS (MALDI-TOF): m/z 461 $[M+H]^+$. HRMS (MALDI-FT): calcd for $C_{24}H_{39}F_3N_2O_3$ $[M]^+$: 460.2907, found: 460.2910.

*4.4.1. Compound **10a**.* White solid. ^{1}H NMR (300 MHz, $CDCl_3$): δ 8.41 (s, 1H), 7.90 (s, 1H), 6.36 (s, 1H), 3.85–3.83 (m, 8H). ^{13}C NMR (100 MHz, $CDCl_3$): δ 153.5 (q, J=37 Hz), 143.2, 140.4, 134.2, 130.5, 115.8 (q, J=286 Hz), 115.2, 104.5, 90.5, 70.4, 56.1. ^{19}F NMR (282 MHz, $CDCl_3$) δ −76.1 (s). MS (ESI): m/z 265 $[M+H]^+$. HRMS (ESI): calcd for $C_{10}H_{12}F_3N_2O_3$ $[M]^+$: 265.0794, found: 265.0802.

*4.4.2. Compound **10c**.* White solid. ^{1}H NMR (300 MHz, $CDCl_3$): δ 8.47 (s, 1H), 7.88 (s, 1H), 6.35 (s, 1H), 3.99–3.88 (m, 6H), 1.80–1.73 (m, 4H), 1.43–1.26 (m, 36H), 0.90–0.85 (m, 6H). ^{13}C NMR (100 MHz, $CDCl_3$): δ 153.4 (q, J=36 Hz), 142.5, 139.9, 134.3, 115.8 (q, J=286 Hz), 115.7, 105.3, 99.8, 69.4, 69.1, 31.8, 29.6 (t), 29.5, 29.4, 29.3, 29.1, 26.0 (d), 22.6 (d), 14.0. ^{19}F NMR (282 MHz, $CDCl_3$): δ −76.3 (s). MS (MALDI-TOF): m/z 573 $[M]^+$. HRMS (MALDI-FT): calcd for $C_{32}H_{55}F_3N_2O_3Na$ $[M]^+$: 595.4057, found: 595.4055.

4.5. Compound 1b

To a stirred solution of compound **10b** (0.26 g, 0.56 mmol) in methanol (10 mL) and tetrahydrofuran (20 mL) was added sodium borohydride (0.21 g, 5.60 mmol) slowly. Stirring was continued for 1 h and then saturated aqueous ammonium chloride solution was added dropwise until no gas was evolved. The mixture was concentrated with a rotavapor and the resulting residue triturated with chloroform (60 mL). The organic phase was washed with aqueous sodium bicarbonate solution (1 N, 20 mL), water (20 mL), and brine (20 mL), and dried over sodium sulfate. The solution was that of crude product **11b**, which was found to be unstable in the air and thus used for the next step without further purification. The solution was concentrated to about 10 mL and then added to a solution of compound **12** (0.50 g, 1.12 mmol) in chloroform (10 mL). To the solution was added *N*-(3-dimethylaminopropyl)-*N*-ethylcarbodiimide hydrochloride (EDC·HCl) (0.24 g, 1.23 mmol). The solution was stirred at room temperature for 24 h and then washed with water (3×5 mL) and brine (10 mL), and dried over sodium sulfate. The solvent was removed with a rotavapor and the resulting slurry was subjected to column chromatography (CH_2Cl_2) to give compound **1b** as a white solid (0.44 g, 65%). ^{1}H NMR (300 MHz, $CDCl_3$): δ 9.13 (s, 2H), 8.19 (s, 2H), 5.37 (d, J=1.5 Hz, 2H), 4.09 (s, 4H), 4.02 (t, J=6.0 Hz, 4H), 3.32–2.98 (m, 2H), 2.45–2.30 (m, 4H), 2.03–1.78 (m, 16H), 1.65–0.80 (m, 90H), 0.68 (s, 6H). ^{13}C NMR (100 MHz, $CDCl_3$): δ 168.0, 141.2, 140.0, 122.8, 122.3, 103.7, 80.3, 69.2, 68.0, 56.7, 56.1, 50.1, 42.3, 39.7, 39.5, 39.0, 37.0, 36.8, 36.1, 35.8, 31.9 (d), 31.8, 29.5 (d), 29.3, 28.3, 28.2, 28.0, 26.1, 24.2, 23.8, 22.8, 22.7, 22.5, 21.0, 19.3, 18.7, 14.1, 11.8. MS (MALDI-FT): m/z 1240.0 $[M+Na]^+$. HRMS (MALDI-FT): calcd for $C_{80}H_{132}N_2O_6Na$ $[M]^+$: 1239.9978, found: 1239.9955.

*4.5.1. Compound **1a**.* White solid. ^{1}H NMR (300 MHz, $CDCl_3$): δ 9.07 (s, 2H), 8.19 (s, 2H), 5.37 (d, J=5.1 Hz, 2H), 4.09 (s, 4H), 3.88 (s, 6H), 3.33–3.26 (m, 2H), 2.46–2.40 (m, 4H), 2.37–1.76 (m, 12H), 1.65–0.85 (m, 64H), 0.67 (s, 6H). ^{13}C NMR ($CDCl_3$): δ 168.3, 141.9, 140.0, 122.6, 122.3, 103.1, 80.5, 68.0, 56.7, 56.4, 56.1, 50.1, 42.3, 39.7, 39.5, 39.0, 37.0, 36.8, 35.8, 31.8, 28.3, 28.2, 28.0, 24.3, 23.8, 22.8, 22.5, 21.0, 19.3, 18.7, 11.8. MS (MALDI-FT): m/z 1043.8 $[M+Na]^+$. HRMS (MALDI-FT): calcd for $C_{66}H_{104}N_2O_6Na$ $[M]^+$: 1043.7787, found: 1043.7754.

*4.5.2. Compound **1c**.* White solid. ^{1}H NMR (300 MHz, $CDCl_3$): δ 9.12 (s, 2H), 8.19 (s, 2H), 5.37 (d, J=1.5 Hz, 2H), 4.06 (s, 4H), 4.02 (t, J=6.0 Hz, 4H), 3.32–2.98 (m, 2H), 2.45–2.30 (m, 4H), 2.03–1.76 (m, 16H), 1.65–0.80 (m, 106H), 0.68 (s, 6H). ^{13}C NMR (75 MHz, $CDCl_3$): δ 168.1, 141.2, 139.9, 122.7, 122.3, 103.7, 80.3, 69.2, 68.0, 56.7, 56.1, 50.1, 42.3, 39.7, 39.5, 39.0, 37.0, 36.8, 36.1, 35.8, 31.9 (d), 31.8, 29.8 (d), 29.7 (d), 29.6, 29.4, 28.4, 28.2, 28.0, 26.2, 24.2, 23.8, 22.8, 22.7, 22.5, 21.0, 19.4, 18.7, 14.1, 11.8. MS (MALDI-TOF): m/z 1353.2 $[M+Na]^+$. Anal. Calcd for $C_{88}H_{148}N_2O_6$: C, 79.46; H, 11.22; N, 2.11. Found: C, 79.57; H, 10.96; N, 2.00.

4.6. Compounds 13a–c

A solution of compounds **10b** (1.70 g, 3.70 mmol), **12** (1.50 g, 3.40 mmol), and EDC·HCl (0.68 g, 3.50 mmol) in chloroform (30 mL) was stirred for 24 h and then another part of chloroform (170 mL) added. The solution was washed with water (3×100 mL) and brine (100 mL), and dried over sodium sulfate. The solvent was then removed and the resulting residue subjected to column chromatography (CH_2Cl_2) to give **13b** as a white solid (1.96 g, 65%). ^{1}H NMR (300 MHz, $CDCl_3$): δ 9.19 (s, 1H), 8.64 (s, 1H), 8.26 (s, 1H), 8.01 (s, 1H), 5.38 (d, J=3.6 Hz, 1H), 4.10–4.00 (m, 6H), 3.35–3.27 (m, 1H), 2.46–2.25 (m, 2H), 2.03–1.77 (m, 10H), 1.61–0.85 (m, 58H), 0.68 (s, 3H). ^{13}C NMR (75 MHz, $CDCl_3$): δ 168.2, 153.9 (q, J=38 Hz), 141.4, 141.2, 139.8, 124.6, 122.4, 120.2, 115.7 (q, J=287 Hz), 103.9, 103.8, 80.3, 69.5, 69.2, 67.9, 56.6, 56.0, 50.0, 42.2, 39.6, 39.4, 38.9, 36.9, 36.7, 36.1, 35.7, 31.9, 31.8 (d), 31.7, 29.4, 29.3, 29.2, 29.1, 29.0, 28.3, 28.2, 28.0, 26.1, 26.0, 24.2, 23.8, 22.8, 22.7, 22.6, 22.5, 21.0, 19.3, 18.6, 14.1, 14.0, 11.8. ^{19}F NMR (282 MHz, $CDCl_3$): δ −76.4 (s). MS (MALDI-FT): m/z 910 $[M+Na]^+$. HRMS (MALDI-FT): calcd for $C_{53}H_{85}F_3N_2O_5Na$ $[M]^+$: 909.6303, found: 909.6330.

*4.6.1. Compound **13a**.* White solid. ^{1}H NMR (300 MHz, $CDCl_3$): δ 9.13 (s, 1H), 8.57 (s, 1H), 8.26 (s, 1H), 8.06 (s, 1H), 5.38 (d, J=4.5 Hz, 1H), 4.10 (s, 2H), 3.91 (s, 3H), 3.90 (s, 3H), 3.36–3.26 (m, 1H), 2.46–2.29 (m, 2H), 2.03–1.77 (m, 6H), 1.56–0.85 (m, 32H), 0.68 (s, 3H). ^{13}C NMR (100 MHz, $CDCl_3$): δ 168.5, 154.1 (q, J=38 Hz), 142.1, 141.7, 139.9, 124.5, 122.4, 120.1, 115.6 (q, J=287 Hz), 103.3, 102.9, 80.5, 67.9, 56.6, 56.4, 56.1, 50.0, 42.2, 39.6, 39.4, 38.9, 36.9, 36.7, 36.1, 35.7, 31.8 (d), 28.3, 28.2, 28.0, 24.2, 23.8 (d), 22.8, 22.5, 21.0, 19.3, 18.6, 11.8. ^{19}F NMR (282 MHz, $CDCl_3$): δ −76.2 (s). MS (MALDI-FT): m/z 713 $[M+Na]^+$. HRMS (MALDI-FT): calcd for $C_{39}H_{57}F_3N_2O_5Na$ $[M]^+$: 713.4112, found: 713.4138.

*4.6.2. Compound **13c**.* White solid. ^{1}H NMR (400 MHz, $CDCl_3$): δ 9.18 (s, 1H), 8.63 (s, 1H), 8.27 (s, 1H), 8.02 (s, 1H), 5.38 (d, J=4.8 Hz, 1H), 4.10–4.01 (m, 6H), 3.34–3.27 (m, 1H), 2.44–2.28 (m, 2H), 2.03–1.76 (m, 10H), 1.60–0.85 (m, 74H), 0.68 (s, 3H). ^{13}C NMR (75 MHz, $CDCl_3$): δ 168.1, 153.8 (q, J=37 Hz), 141.4, 141.1, 139.7, 124.6, 122.3, 120.2, 115.7 (q, J=287 Hz), 103.9, 103.8, 80.3, 69.4, 69.2, 67.8, 56.6, 56.1, 50.0, 42.2, 39.6, 39.4, 38.9, 36.9, 36.7, 36.1, 35.7, 31.9 (d), 31.8 (d), 29.8, 29.7 (d), 29.6, 29.5, 29.4, 29.3, 29.0, 28.3, 28.1, 27.9, 26.2, 26.0, 24.2, 23.8, 22.7, 22.6 (d), 22.5, 21.0, 19.2, 18.6, 14.0, 11.7. ^{19}F NMR (376 MHz, $CDCl_3$): δ −76.0 (s). MS (MALDI-FT): m/z 1021.8 $[M+Na]^+$. HRMS (MALDI-FT): calcd for $C_{61}H_{101}F_3N_2O_5Na$ $[M]^+$: 1021.7555, found: 1021.7556.

4.7. Compound 14c

To a stirred solution of compound **13b** (0.89 g, 1.00 mmol) in methanol (100 mL) and tetrahydrofuran (200 mL) was added

sodium borohydride (0.57 g, 15.0 mmol). The solution was stirred for 2 h and then saturated aqueous ammonium chloride solution added dropwise until no gas was evolved. The mixture was concentrated with a rotavapor and the obtained slurry triturated with ethyl acetate (200 mL). The organic phase was washed with water (3×70 mL) and brine (70 mL), and dried over sodium sulfate. After the solvent was removed in vacuo, the resulting residue was subjected to flash chromatography (dichloromethane/AcOEt 10:1) to give compound **14b** as a white solid (0.76 g, 96%). ^{1}H NMR (300 MHz, $CDCl_3$): δ 8.92 (s, 1H), 8.05 (s, 1H), 6.34 (s, 1H), 5.39–5.35 (m, 1H), 4.07 (s, 2H), 3.98 (t, J=6.4 Hz, 2H), 3.91 (t, J=6.8 Hz, 2H), 3.68 (br, 2H), 3.33–3.25 (m, 1H), 2.44–2.26 (m, 2H), 2.03–1.77 (m, 10H), 1.61–0.85 (m, 58H), 0.68 (s, 3H). ^{13}C NMR (75 MHz, $CDCl_3$): δ 167.3, 142.1, 140.0, 139.9, 132.2, 122.2, 118.4, 105.3, 100.1, 80.2, 69.12, 69.07, 67.9, 56.6, 56.1, 50.0, 42.2, 39.7, 39.4, 39.0, 36.9, 36.7, 36.1, 35.7, 31.9, 31.8 (t), 29.6, 29.4 (t), 29.3, 29.2, 28.3, 28.2, 27.9, 26.1 (d), 24.2, 23.8, 22.8, 22.6 (d), 22.5, 21.0, 19.3, 18.6, 14.08, 14.05, 11.8. MS (MALDI-FT): m/z 790.7 $[M]^+$, 813.6 $[M+Na]^+$. HRMS (MALDI-FT): calcd for $C_{51}H_{86}N_2O_4Na$: 813.6480, found: 813.6474.

4.7.1. Compound ***14a***. White solid. ^{1}H NMR (300 MHz, $CDCl_3$): δ 8.84 (s, 1H), 8.01 (s, 1H), 6.35 (s, 1H), 5.39–5.35 (m, 1H), 4.07 (s, 2H), 3.83 (s, 3H), 3.79 (s, 3H), 3.36–3.26 (m, 1H), 2.46–2.29 (m, 2H), 2.03–1.77 (m, 6H), 1.56–0.85 (m, 32H), 0.68 (s, 3H). ^{13}C NMR (100 MHz, $CDCl_3$): δ 167.6, 142.9, 140.7, 140.1, 132.2, 122.3, 118.1, 104.6, 99.3, 80.4, 68.0, 56.7, 56.3, 56.3, 56.1, 50.0, 42.3, 39.7, 39.5, 39.0, 37.0, 36.8, 36.1, 35.8, 31.9, 31.8, 28.3, 28.2, 28.0, 24.2, 23.8 (d), 22.8, 22.5, 21.0, 19.3, 18.6, 11.8. MS (MALDI-FT): m/z 594.4 $[M]^+$, 617.4 $[M+Na]^+$. HRMS (MALDI-FT): calcd for $C_{37}H_{58}N_2O_4Na$: 617.4289, found: 617.4282.

4.7.2. Compound ***14c***. White solid. ^{1}H NMR (400 MHz, $CDCl_3$): δ 8.91 (s, 1H), 8.05 (s, 1H), 6.34 (s, 1H), 5.39–5.34 (m, 1H), 4.07 (s, 1H), 3.97 (t, J=6.8 Hz, 2H), 3.91 (t, J=6.8 Hz, 2H), 3.69 (br, 2H), 3.33–3.25 (m, 1H), 2.44–2.28 (m, 2H), 2.03–1.76 (m, 10H), 1.60–0.85 (m, 74H), 0.68 (s, 3H). ^{13}C NMR (75 MHz, $CDCl_3$): δ 167.3, 142.2, 140.1, 140.0, 132.2, 122.2, 118.4, 105.4, 100.2, 80.2, 69.2, 69.1, 68.0, 56.7, 56.1, 50.0, 42.2, 39.7, 39.5, 39.0, 36.9, 36.7, 36.1, 35.7, 31.9, 31.9, 31.8, 29.8 (d), 29.7 (d), 29.6 (d), 29.4, 29.4, 29.3, 28.3, 28.1, 28.0, 26.2, 26.1, 24.2, 23.8, 22.8, 22.7, 22.5, 21.0, 19.3, 18.6, 14.1, 11.8. MS (MALDI-FT): m/z 902.8 $[M]^+$, 925.8 $[M+Na]^+$. HRMS (MALDI-FT): calcd for $C_{59}H_{102}N_2O_4Na$: 925.7732, found: 925.7719.

4.8. Compounds 2a–i

To a stirred solution of compounds **14b** (0.28 g, 0.35 mmol) and **15b** (51 mg, 0.12 mmol) in chloroform (5 mL), cooled in an ice-bath, was added EDC·HCl (73 mg, 0.39 mmol) slowly. The solution was stirred at room temperature for 48 h and then another part of chloroform (35 mL) was added. The solution was washed with water (3×20 mL) and brine (20 mL), and dried over sodium sulfate. After the solvent was removed in vacuo, the resulting residue was subjected to flash chromatography and further recrystallized from dichloromethane and ethyl acetate. Compound **2e** was obtained as a yellow solid (0.16 g, 66%). ^{1}H NMR (400 MHz, $CDCl_3$): δ 10.50 (s, 2H), 9.16 (s, 2H), 8.39 (s, 2H), 8.26 (s, 2H), 7.96 (s, 2H), 5.38 (s, 2H), 4.28 (t, J=6.8 Hz, 4H), 4.11–4.09 (m, 12H), 3.36–3.28 (m, 2H), 2.47–2.29 (m, 4H), 2.04–1.76 (m, 24H), 1.67–0.82 (m, 142H), 0.692 (s, 6H). ^{13}C NMR (100 MHz, $CDCl_3$): δ 168.0, 162.1, 150.7, 141.7, 141.3, 140.0, 125.9, 123.9, 123.0, 122.3, 116.6, 105.1, 104.3, 80.4, 70.4, 69.7, 69.1, 68.0, 56.7, 56.1, 50.1, 42.3, 39.7, 39.5, 39.0, 36.8, 36.2, 35.8, 32.0, 31.9, 31.8 (d), 31.7, 29.6, 29.5, 29.4, 29.3 (d), 29.2, 29.0, 28.4, 28.2, 28.0, 26.2, 25.9, 25.8, 24.3, 23.8, 22.8, 22.7, 22.6 (d), 21.0, 19.3, 18.7, 14.1, 14.0, 11.8. MS (MALDI-FT): m/z 1990.6 $[M+Na]^+$. HRMS (MALDI-FT): calcd for $C_{126}H_{206}N_4O_{12}Na$ $[M]^+$: 1990.5524, found: 1990.5558.

4.8.1. Compound ***2a***. Yellow solid (72%). ^{1}H NMR (300 MHz, $CDCl_3$): δ 10.89 (s, 2H), 9.09 (s, 2H), 8.46 (s, 2H), 8.24 (s, 2H), 8.02 (s, 2H), 5.38 (d, J=5.1 Hz, 2H), 4.14 (s, 6H), 4.11 (s, 4H), 3.97 (s, 6H), 3.95 (s, 6H), 3.35–3.27 (m, 2H), 2.47–2.29 (m, 4H), 2.03–1.76 (m, 12H), 1.59–0.83 (m, 64H), 0.68 (s, 6H). ^{13}C NMR (75 MHz, $CDCl_3$): δ 168.3, 161.6, 151.5, 142.2, 142.0, 140.0, 125.2, 123.9, 122.7, 122.4, 115.1, 103.7, 103.1, 80.5, 68.0, 56.7, 56.3, 56.1, 50.1, 42.3, 39.7, 39.5, 39.0, 37.0, 36.8, 36.2, 35.8, 31.9, 31.8, 28.3, 28.2, 28.0, 24.3, 23.8, 22.8, 22.5, 21.1, 19.3, 18.7, 11.8. MS (MALDI-TOF): m/z 1402.5 $[M+Na]^+$. Anal. Calcd for $C_{84}H_{122}N_4O_{12}$: C, 73.11; H, 8.91; N, 4.06. Found: C, 72.71; H, 9.03; N, 3.79.

4.8.2. Compound ***2b***. Yellow solid (68%). ^{1}H NMR (400 MHz, $CDCl_3$): δ 10.66 (s, 2H), 9.10 (s, 2H), 8.50 (s, 2H), 8.24 (s, 2H), 8.00 (s, 2H), 5.38 (d, J=3.9 Hz, 2H), 4.27 (t, J=6.9 Hz, 4H), 4.11 (s, 4H), 3.94 (s, 6H), 3.92 (s, 6H), 3.35–3.28 (m, 2H), 2.48–2.30 (m, 4H), 2.00–1.77 (m, 16H), 1.60–0.85 (m, 90H), 0.68 (s, 6H); ^{13}C NMR (100 MHz, $CDCl_3$) δ 168.1, 161.9, 150.7, 142.2, 141.6, 139.9, 125.1, 123.6, 122.6, 122.2, 116.0, 104.1, 102.7, 80.4, 70.2, 67.9, 56.6, 56.3, 56.1, 55.9, 50.0, 42.2, 39.6, 39.4, 38.9, 36.9, 36.7, 36.1, 35.7, 31.80, 31.77, 31.7, 29.3, 29.20, 29.16, 28.2, 28.1, 28.0, 25.7, 24.2, 23.8, 22.7, 22.6, 22.5, 21.0, 19.3, 18.6, 14.0, 11.8. MS (MALDI-FT): 1598.1 $[M+Na]^+$. HRMS (MALDI-FT): calcd for $C_{98}H_{150}N_4O_{12}Na$ $[M]^+$: 1598.1142, found: 1598.1142. Anal. Calcd for $C_{98}H_{150}N_4O_{12}$: C, 74.67; H, 9.59; N, 3.55. Found: C, 74.55; H, 9.47; N, 3.66.

4.8.3. Compound ***2c***. Yellow solid (69%). ^{1}H NMR (300 MHz, $CDCl_3$): δ 10.66 (s, 2H), 9.10 (s, 2H), 8.50 (s, 2H), 8.24 (s, 2H), 8.00 (s, 2H), 5.38 (d, J=5.1 Hz, 2H), 4.27 (t, J=6.9 Hz, 4H), 4.11 (s, 4H), 3.94 (s, 6H), 3.92 (s, 6H), 3.35–3.28 (m, 2H), 2.48–2.30 (m, 4H), 2.02–1.80 (m, 16H), 1.60–0.85 (m, 106H), 0.68 (s, 6H). ^{13}C NMR (100 MHz, $CDCl_3$): δ 168.2, 162.0, 150.7, 142.3, 141.7, 140.0, 125.2, 123.6, 122.7, 122.3, 116.0, 104.1, 102.7, 80.4, 70.2, 68.0, 56.6, 56.3, 56.1, 56.0, 50.0, 42.2, 39.7, 39.4, 38.9, 36.9, 36.7, 36.1, 35.7, 31.9, 31.8, 29.6 (d), 29.5, 29.4, 29.3, 29.1, 28.3, 28.2, 28.0, 25.7, 24.2, 23.8, 22.8, 22.6, 22.5, 21.0, 19.3, 18.6, 14.1, 11.8. MS (MALDI-FT): m/z 1710.2 $[M+Na]^+$. HRMS (MALDI-FT): calcd for $C_{106}H_{166}N_4O_{12}Na$ $[M]^+$: 1710.2394, found: 1710.2377. Anal. Calcd for $C_{106}H_{166}N_4O_{12}$: C, 75.40; H, 9.91; N, 3.32. Found: C, 75.12; H, 9.94; N, 3.17.

4.8.4. Compound ***2d***. Yellow solid (64%). ^{1}H NMR (400 MHz, $CDCl_3$): δ 10.69 (s, 2H), 9.17 (s, 2H), 8.46 (s, 2H), 8.26 (s, 2H), 8.03 (s, 2H), 5.38 (d, J=4.4 Hz, 2H), 4.11–4.08 (m, 18H), 3.35–3.29 (m, 2H), 2.46–2.29 (m, 4H), 2.02–1.78 (m, 16H), 1.60–0.84 (m, 114H), 0.68 (s, 6H). ^{13}C NMR (100 MHz, $CDCl_3$): δ 167.9, 161.5, 151.4, 141.5, 141.1, 139.9, 125.2, 123.7, 122.9, 122.3, 115.2, 104.6, 103.6, 80.2, 69.3, 69.1, 67.9, 56.6, 56.1, 50.0, 42.2, 39.7, 39.4, 39.0, 36.9, 36.7, 36.1, 35.7, 31.9, 31.8, 31.7, 31.6, 29.6, 29.5, 29.4, 29.3, 29.2, 28.3, 28.2, 28.0, 26.2, 25.9, 24.2, 23.8, 22.8, 22.7, 22.6, 22.5, 21.0, 19.3, 18.6, 14.1, 14.0, 11.8. MS (MALDI-FT): m/z 1794.3 $[M+Na]^+$. HRMS (MALDI-FT): calcd for $C_{112}H_{178}N_4O_{12}Na$ $[M]^+$: 1794.3334, found: 1794.3334.

4.8.5. Compound ***2f***. Yellow solid (66%). ^{1}H NMR (300 MHz, $CDCl_3$): δ 10.51 (s, 2H), 9.17 (s, 2H), 8.40 (s, 2H), 8.27 (s, 2H), 7.97 (s, 2H), 5.38 (d, J=3.6 Hz, 2H), 4.28 (t, J=6.6 Hz, 4H), 4.11 (br, 12H), 3.32 (m, 2H), 2.43–2.31 (m, 4H), 2.04–1.77 (m, 24H), 1.67–0.82 (m, 158H), 0.69 (s, 6H). ^{13}C NMR (75 MHz, $CDCl_3$): δ 168.1, 162.2, 150.8, 141.8, 141.3, 140.0, 126.0, 123.9, 123.1, 122.4, 116.6, 105.1, 104.4, 80.4, 70.5, 69.7, 69.2, 56.7, 56.2, 50.1, 42.3, 39.5, 36.8, 32.0, 31.9, 31.8, 29.6, 29.42, 29.35, 28.0, 26.2, 25.9, 25.8, 22.8, 22.7, 22.65, 22.57, 19.4, 18.7, 14.1, 14.1, 11.9. MS (MALDI-FT): m/z 2102.7 $[M+Na]^+$. HRMS (MALDI-FT): calcd for $C_{134}H_{222}N_4O_{12}Na$ $[M]^+$: 2102.6776, found: 2102.6739. Anal. Calcd for $C_{134}H_{222}N_4O_{12}$: C, 77.33; H, 10.75; N, 2.69. Found: C, 77.57; H, 10.77; N, 2.49.

4.8.6. Compound ***2g***. Yellow solid (62%). ^{1}H NMR (300 MHz, $CDCl_3$): δ 10.67 (s, 2H), 9.17 (s, 2H), 8.46 (s, 2H), 8.26 (s, 2H), 8.02 (s, 2H),

5.38 (d, J=4.4 Hz, 2H), 4.11 (br, 18H), 3.36–3.26 (m, 2H), 2.47–2.26 (m, 4H), 2.00–1.84 (m, 16H), 1.60–0.85 (m, 146H), 0.68 (s, 6H). ^{13}C NMR (100 MHz, $CDCl_3$): δ 168.0, 161.6, 151.4, 141.6, 141.2, 139.9, 125.3, 123.8, 122.9, 122.3, 115.2, 104.6, 103.6, 80.3, 69.3, 69.1, 68.0, 56.7, 56.1, 50.0, 42.2, 39.7, 39.4, 39.0, 36.9, 36.7, 36.1, 35.7, 31.9, 31.8, 31.7, 31.6, 29.6, 29.5, 29.4, 29.3, 29.2, 28.3, 28.2, 28.0, 26.2, 25.9, 24.2, 23.8, 22.8, 22.7, 22.6, 22.5, 21.0, 19.3, 18.6, 14.1, 14.0, 11.8. MS (MALDI-FT): m/z 2018.6 $[M+Na]^+$. HRMS (MALDI-FT): calcd for $C_{128}H_{210}N_4O_{12}Na$ $[M]^+$: 2018.5838, found: 2018.5821.

4.8.7. Compound ***2h***. Yellow solid (68%). ^{1}H NMR (400 MHz, $CDCl_3$): δ 10.51 (s, 2H), 9.16 (s, 2H), 8.39 (s, 2H), 8.26 (s, 2H), 7.96 (s, 2H), 5.38 (s, 2H), 4.28 (t, J=6.8 Hz, 4H), 4.10–4.07 (m, 12H), 3.36–3.27 (m, 2H), 2.47–2.28 (m, 4H), 2.03–1.77 (m, 24H), 1.61–0.82 (m, 174H), 0.68 (s, 6H). ^{13}C NMR (100 MHz, $CDCl_3$): δ 168.0, 162.1, 150.7, 141.7, 141.3, 140.0, 125.9, 123.9, 123.0, 122.3, 116.6, 105.1, 104.3, 80.4, 70.4, 69.6, 69.1, 68.0, 56.7, 56.1, 50.1, 42.3, 39.7, 39.5, 39.0, 37.0, 36.7, 36.1, 35.8, 31.93, 31.9, 31.7, 29.8, 28.7, 29.6, 29.4 (d), 29.3 (d), 29.2, 28.9, 28.4, 28.2, 28.0, 26.2, 25.9, 25.8, 24.2, 23.8, 22.8, 22.7 (d), 22.6, 22.5, 21.0, 19.3, 18.7, 14.1 (d), 14.0, 11.8. MS (MALDI-FT): m/z 2217.8 $[M+Na]^+$. HRMS (MALDI-FT): calcd for $C_{142}H_{238}N_4O_{12}Na$ $[M]^+$: 2214.8028, found: 2214.8086.

4.8.8. Compound ***2i***. Yellow solid (61%). ^{1}H NMR (300 MHz, $CDCl_3$): δ 10.51 (s, 2H), 9.16 (s, 2H), 8.39 (s, 2H), 8.26 (s, 2H), 7.96 (s, 2H), 5.34 (d, J=5.4 Hz, 2H), 4.28 (t, J=6.3 Hz, 4H), 4.11–4.08 (m, 12H), 3.34–3.27 (m, 2H), 2.46–2.30 (m, 4H), 1.99–1.74 (m, 24H), 1.67–0.83 (m, 190H), 0.68 (s, 6H). ^{13}C NMR (75 MHz, $CDCl_3$): δ 168.0, 162.1, 150.7, 141.7, 141.2, 139.9, 125.9, 123.8, 123.0, 122.3, 116.6, 105.0, 104.3, 80.3, 70.4, 69.6, 69.1, 68.0, 56.7, 56.1, 50.0, 42.3, 39.7, 39.5, 39.0, 37.0, 36.7, 36.1, 35.8, 31.9, 31.9, 31.8, 29.8 (d), 29.7 (t), 29.6, 29.4 (d), 29.3 (d), 28.9, 28.4, 28.2, 28.0, 26.2, 25.8, 25.7, 24.2, 23.8, 22.8, 22.7, 22.5, 21.0, 19.3, 18.7, 14.1, 11.8. MS (MALDI-FT): m/z 2327.0 $[M+Na]^+$. HRMS (MALDI-FT): calcd for $C_{150}H_{254}N_4O_{12}Na$ $[M]^+$: 2326.9280, found: 2326.9317. Anal. Calcd for $C_{150}H_{254}N_4O_{12}$: C, 78.14; H, 11.10; N, 2.43. Found: C, 78.35; H, 11.00; N, 2.19.

4.9. Compound 16

A solution of compound **15** (5.00 g, 8.50 mmol) and potassium hydroxide (0.47 g, 8.50 mmol) in ethanol (300 mL) was heated under reflux for 24 h and then concentrated in vacuo. The resulting slurry was treated with dilute hydrochloric acid (0.5 N, 10 mL) and the mixture extracted with chloroform (3×100 mL). The organic phases were combined and washed with water (2×100 mL) and brine (100 mL), and dried over sodium sulfate. Upon removal of the solvent, the crude product was recrystallized from petroleum ether (60–90 °C) to give compound **16** as a white solid (3.20 g, 67%). ^{1}H NMR (300 MHz, $CDCl_3$): δ 11.22 (s, 1H), 7.74 (s, 1H), 7.42 (s, 1H), 4.39 (q, J=7.2 Hz, 2H), 4.23 (t, J=6.4 Hz, 2H), 4.04 (t, J=6.3 Hz, 2H), 1.92–1.77 (m, 4H), 1.48–1.25 (m, 39H), 0.89–0.84 (m, 6H). ^{13}C NMR (100 MHz, $CDCl_3$): δ 165.6, 164.6, 152.7, 150.5, 126.2, 120.8, 117.4, 115.7, 71.0, 69.5, 61.5, 31.8, 29.6, 29.5, 29.4, 29.34, 29.26, 29.10, 29.07, 28.8, 25.8, 25.7, 22.6, 14.2, 14.0. MS (MALDI-FT): m/z 585.4 $[M+Na]^+$. HRMS (MALDI-FT): calcd for $C_{34}H_{58}O_6Na$ $[M]^+$: 585.4126, found: 585.4145. Anal. Calcd for $C_{34}H_{58}O_6$: C, 72.56; H, 10.36. Found: C, 72.80; H, 10.52.

4.10. Compound 17

To a stirred solution of compound **16** (0.22 g, 0.40 mmol) in chloroform (5 mL) were added DMF (0.05 mL) and oxalyl chloride (1.00 mL). The solution was stirred at room temperature for 1 h and then concentrated under reduced pressure. The obtained residue was dissolved again in chloroform (6 mL) and the solution added slowly to a stirred solution of **11c** (94 mg, 0.20 mmol) and triethylamine (0.06 mL, 0.06 mmol) in chloroform (10 mL). Stirring was continued for 12 h and the solution washed with aqueous hydrochloric acid (1 N, 10 mL), water (2×10 mL), and brine (10 mL), and dried over sodium sulfate. The solvent was then removed in vacuo and the resulting residue was subjected to flash chromatography (CH_2Cl_2) to give compound **17** as a yellow solid (0.15 g, 48%). ^{1}H NMR (300 MHz, $CDCl_3$): δ 10.48 (s, 2H), 8.45 (s, 2H), 7.86 (s, 2H), 7.45 (s, 2H), 4.39 (q, J=7.1 Hz, 4H), 4.21 (t, J=7.0 Hz, 4H), 4.13 (t, J=7.0 Hz, 4H), 4.08 (t, J=7.0 Hz, 4H), 1.91–1.77 (m, 12H), 1.47–1.22 (m, 114H). 0.89–0.83 (m, 18H). ^{13}C NMR (75 MHz, $CDCl_3$): δ 166.1, 162.2, 152.6, 149.8, 141.7, 126.5, 124.0, 123.9, 116.6, 116.4, 105.4, 70.7, 69.5, 61.3, 31.9, 29.6, 29.4, 29.3, 29.2, 28.9, 25.93, 25.87, 25.7, 22.6, 14.2, 14.1. MS (MALDI-FT): m/z 1566.3 $[M+H]^+$, 1588.2 $[M+Na]^+$. HRMS (MALDI-FT): calcd for $C_{98}H_{168}N_2O_{12}Na$ $[M]^+$: 1588.2489, found: 1588.2443.

4.11. Compound 18

A solution of compound **17** (0.12 g, 0.077 mmol) and potassium hydroxide (13 mg, 0.23 mmol) in ethanol (30 mL) and water (15 mL) was heated under reflux for 48 h and then neutralized with hydrochloric acid to pH=5. The mixture was concentrated in vacuo and the resulting solid washed with water thoroughly to give compound **18** as a white solid (0.11 g, 94%). ^{1}H NMR (300 MHz, $CDCl_3$): δ 11.22 (br, 2H), 10.49 (s, 2H), 8.42 (s, 2H), 7.99 (s, 2H), 7.86 (s, 2H), 4.32 (t, J=6.6 Hz, 4H), 4.28 (t, J=6.6 Hz, 4H), 4.14 (t, J=6.6 Hz, 4H), 1.91–1.78 (m, 12H), 1.57–1.22 (m, 108H), 0.89–0.82 (m, 18H). ^{13}C NMR (100 MHz, $CDCl_3$): δ 164.6, 161.4, 151.4, 151.0, 141.7, 127.9, 124.0, 120.6, 117.6, 116.2, 105.5, 70.9, 70.6, 69.5, 31.8, 30.2, 29.6, 29.5, 29.4, 29.3, 29.1, 28.9, 28.8, 25.9, 25.71, 25.67, 22.6, 14.0. MS (MALDI-FT): m/z 1509.2 $[M]^+$, 1532.2 $[M+Na]^+$; HRMS (MALDI-FT): calcd for $C_{94}H_{160}N_2O_{12}Na$ $[M]^+$: 1532.1863, found: 1532.1872.

4.12. Compound 3

To a stirred solution of compounds **14c** (0.32 g, 0.35 mmol) and **18** (0.18 g, 0.12 mmol) in chloroform, cooled in an ice-bath, was added EDC·HCl (73 mg, 0.39 mmol). The mixture was stirred at room temperature for 48 h and then diluted with chloroform (35 mL). The solution was successively washed with water (3×20 mL) and brine (20 mL), and dried over sodium sulfate. After the solvent was removed in vacuo, the resulting residue was subjected to flash chromatography (CH_2Cl_2) to give a solid, which was recrystallized from dichloromethane and ethyl acetate to afford compound **3** as a yellow solid (0.18 g, 45%). ^{1}H NMR (300 MHz, $CDCl_3$): δ 10.53 (s, 2H), 10.52 (s, 2H), 9.17 (s, 2H), 8.45 (s, 2H), 8.39 (s, 2H), 8.26 (s, 2H), 7.97 (s, 4H), 5.38 (d, J=4.5 Hz, 2H), 4.29 (t, J=6.9 Hz, 8H), 4.17–4.08 (m, 16H), 3.37–3.27 (m, 2H), 2.47–2.27 (m, 4H), 2.00–1.75 (m, 32H), 1.64–0.83 (m, 274H), 0.68 (s, 6H). ^{13}C NMR (100 MHz, $CDCl_3$): δ 168.0, 162.1, 150.7, 150.6, 141.8, 141.7, 141.2, 140.0, 126.0, 125.9, 124.1, 123.8, 123.0, 122.3, 116.6, 105.6, 105.0, 104.3, 80.3, 70.4, 69.6 (d), 69.1, 68.0, 56.6, 56.1, 50.0, 42.2, 39.7, 39.4, 39.0, 36.9, 36.7, 36.1, 35.7, 31.9 (d), 29.8 (d), 29.7, 29.6, 29.5, 29.4 (d), 29.3, 28.9, 28.3, 28.2, 28.0, 26.2, 25.9, 25.8, 25.7, 24.2, 23.8, 22.8, 22.6, 22.5, 21.0, 19.3, 18.6, 14.1, 11.8. MS (MALDI-FT): m/z 3301.7 $[M+Na]^+$. HRMS (MALDI-FT): calcd for $C_{212}H_{360}N_6O_{18}Na$ $[M]^+$: 3301.7331, found: 3301.7334.

4.13. Compound 4

To a stirred solution of compounds **7c** (0.28 g, 0.60 mmol) and **12** (0.27 g, 0.60 mmol) in chloroform (5 mL) were added EDC·HCl (0.32 g, 1.70 mmol) and 1-hydroxybenzotriazole 5-amino tetrazole (HOBT, 10 mg). The solution was stirred for 48 h and then diluted with chloroform (50 mL). The solution was successively washed with water (3×20 mL) and brine (20 mL), and dried over sodium sulfate. Upon removal of the solvent with a rotavapor, the resulting residue was subjected to flash chromatography (petroleum ether/dichloromethane 1:1). The obtained product was further recrystallized from petroleum ether and dichloromethane to give compound **4** as

a white solid (0.32 g, 60%). ^{1}H NMR (300 MHz, $CDCl_3$): δ 9.16 (s, 1H), 8.15 (d, J=3.0 Hz, 1H), 6.77 (d, J=8.4 Hz, 1H), 6.55 (dd, J_1=3.0 Hz, J_2=9.0 Hz, 1H), 5.37 (d, J=4.2 Hz, 1H), 4.10 (s, 2H), 3.96–3.92 (m, 4H), 3.35–3.25 (m, 1H), 2.45–2.26 (m, 2H), 2.04–1.70 (m, 10H), 1.61–0.85 (m, 74H), 0.68 (s, 3H). ^{13}C NMR (75 MHz, $CDCl_3$): δ 168.2, 153.4, 141.776, 140.0, 128.0, 122.3, 111.8, 109.4, 106.4, 80.4, 77.33, 77.0, 76.7, 69.3, 68.6, 68.1, 56.7, 50.2, 42.3, 39.8, 39.5, 39.0, 36.8, 36.2, 35.8, 32.0, 31.9, 29.81, 29.78, 29.75, 29.68, 29.64, 29.60, 29.44, 29.42, 29.36, 28.4, 28.2, 28.0, 26.2, 26.1, 24.3, 23.8, 22.8, 22.7, 22.6, 21.1, 19.4, 18.7, 14.1, 11.8. MS (MALDI-TOF): m/z 888 $[M]^+$. Anal. Calcd for $C_{59}H_{101}NO_4$: C, 79.76; H, 11.46; N, 1.58. Found: C, 79.91; H, 11.22; N, 1.50.

Acknowledgements

We thank National Natural Science Foundation of China (Nos. 20732007, 20921091, 20872167, 20974118), Ministry of Science and Technology of China (2007CB808001), and Science and Technology Commission of Shanghai Municipality (09XD1405300) for financial support.

Supplementary data

Supplementary data associated with this article can be found in the online version, at doi:10.1016/j.tet.2010.11.046.

References and notes

1. Chandrasekhar, S. *Liquid Crystals*; Cambridge University Press: Cambridge, 1994; 480 pp.
2. Imrie, C. T.; Luckhurst, G. R. In *Handbook of Liquid Crystals*; Demus, D., Goodby, J., Gray, G. W., Spiess, H.-W., Vill, V., Eds.; Wiley-VCH: Weinheim, 1998; Vol. 2B.
3. Xie, P.; Zhang, R. *J. Mater. Chem.* **2005**, *15*, 2529–2550.
4. Hird, M. *Chem. Soc. Rev.* **2007**, *36*, 2070–2095.
5. Hamley, I. W.; Castelletto, V. *Angew. Chem., Int. Ed.* **2007**, *46*, 4442–4455.
6. Matharu, A. S.; Jeeva, S.; Ramanujam, P. S. *Chem. Soc. Rev.* **2007**, *36*, 1868–1880.
7. Bruce, D. W. *Struct. Bonding* **2008**, *126*, 161–180.
8. Funahashi, M.; Shimura, H.; Yoshio, M.; Kato, T. *Struct. Bonding* **2008**, *128*, 151–179.
9. Saez, I. M.; Goodby, J. W. *Struct. Bonding* **2008**, *128*, 1–62.
10. Binnemans, K. *J. Mater. Chem.* **2009**, *19*, 448–453.
11. Bisoyi, H. K.; Kumar, S. *Chem. Soc. Rev.* **2010**, *39*, 264–285.
12. Shinkai, S.; Murata, K. *J. Mater. Chem.* **1998**, *8*, 485–495.
13. Jin, J.-I. *Mol. Cryst. Liq. Cryst. Sci. Technol., Sect. A* **1995**, *267*, 249–265.
14. Yelamaggad, C. V.; Shanker, G.; Hiremath, U. S.; Prasad, S. K. *J. Mater. Chem.* **2008**, *18*, 2927–2949.
15. Imrie, C. T.; Henderson, P. A. *Chem. Soc. Rev.* **2007**, *36*, 2096–2124.
16. Mallia, V. A.; Tamaoki, N. *Chem. Soc. Rev.* **2004**, *33*, 76–84.
17. Tamaoki, N.; Parfenov, A. V.; Masaki, A.; Matsuda, H. *Adv. Mater.* **1997**, *9*, 1102–1104.
18. Tamaoki, N.; Kruk, G.; Matsuda, H. *J. Mater. Chem.* **1999**, *9*, 2381–2384.
19. Tamaoki, N. *Adv. Mater.* **2001**, *13*, 1135–1147.
20. Yang, Y.-L.; Chan, Q.-L.; Ma, X.-J.; Deng, K.; Shen, Y.-T.; Feng, X.-Z.; Wang, C. *Angew. Chem., Int. Ed.* **2006**, *45*, 6889–6893.
21. Gong, B. *Chem.—Eur. J.* **2001**, *7*, 4336–4342.
22. Huc, I. *Eur. J. Org. Chem.* **2004**, 17–29.
23. Li, Z.-T.; Hou, J.-L.; Li, C. *Acc. Chem. Res.* **2008**, *41*, 1343–1353.
24. Saraogi, I.; Hamilton, A. D. *Chem. Soc. Rev.* **2009**, *38*, 1726–1743.
25. Li, Z.-T.; Hou, J.-L.; Li, C.; Yi, H.-P. *Chem. Asian J.* **2006**, *1*, 766–778.
26. Zhao, X.; Li, Z.-T. *Chem. Commun.* **2010**, *46*, 1601–1616.
27. Wu, Z.-Q.; Shao, X.-B.; Li, C.; Hou, J.-L.; Wang, K.; Jiang, X.-K.; Li, Z.-T. *J. Am. Chem. Soc.* **2005**, *127*, 17460–17468.
28. Xiao, Z.-Y.; Hou, J.-L.; Jiang, X.-K.; Li, Z.-T.; Ma, Z. *Tetrahedron* **2009**, *65*, 10182–10191.
29. Wu, Z.-Q.; Jiang, X.-K.; Zhu, S.-Z.; Li, Z.-T. *Org. Lett.* **2004**, *6*, 229–232.
30. Wu, Z.-Q.; Jiang, X.-K.; Li, Z.-T. *Tetrahedron Lett.* **2005**, *46*, 8067–8070.
31. Lion, C.; Baudry, R.; Hedayatullah, M.; Conceicao, L. D.; Genard, M.; Maignan, J. *J. Heterocycl. Chem.* **2002**, *39*, 125–130.
32. Hussey, S. L.; He, K.; Peterson, B. R. *Org. Lett.* **2002**, *4*, 415–418.
33. Demus, D.; Richter, L. *Textures of Liquid Crystals*; Chemie: Weinheim, 1978.
34. Demus, D.; Goodby, J. W.; Gray, G. W.; Spiess, H.-W.; Vill, V. *Handbook of Liquid Crystals: Fundamental*; WILEY-VCH: 1998; Vol. 1.